Detecting eccentricity faults in a PMSM in non-stationary conditions

Detección de fallo de excentricidad en PMSM bajo condiciones no estacionarias

Javier **Rosero** García[1], José Luis **Romeral**[2], Esteban **Rosero** García[3]

RESUMEN

Los motores síncronos de imanes permanentes son ampliamente usados en aplicaciones que requieren alto rendimiento y resistencia como automatización industrial, aeroespacial y automotriz. Este artículo presenta un estudio de motor síncrono de imanes permanentes (PMSM) en condición de falla de excentricidad. En este contexto, la monitorización y detección de fallas de PMSM proporcionan un valor añadido y están adquiriendo una importancia cada vez mayor. En este artículo se investiga el efecto de la excentricidad en el espectro de corriente de motores PMSM con el fin de desarrollar un esquema eficaz de supervisión. Para poder realizar el estudio se usa el análisis de elementos finitos (FEA) de dos dimensiones (2-D). Se investigan los armónicos inducidos en la corriente de estator por condición de fallas y se usa el análisis avanzado de señales por medio de la transformada Wavelet continua y discreta. Los resultados de simulación y experimentales son presentados para corroborar el método propuesto en un amplio rango de velocidad de operación del motor y proporcionan una herramienta eficaz para el diagnóstico de condición de falla de un PMSM.

Palabras clave: motor síncrono de imanes permanentes (PMSM), monitoreo, diagnóstico de fallas, excentricidad, fallas mecánicas, análisis de corriente de estator (MCIA), análisis Wavelet, análisis de elementos finitos (FEA).

ABSTRACT

Permanent magnet alternating current machines are being widely used in applications demanding high and rugged performance, such as industrial automation and the aerospace and automotive industries. This paper presents a study of a permanent magnet synchronous machine (PMSM) running in eccentricity; these machines' condition monitoring and fault detection would provide added value and they are also assuming growing importance. This paper investigates the effect of eccentricity faults on PMSM motors' current spectrum with a view to developing an effective condition-monitoring scheme using two-dimensional (2-D) finite element analysis (FEA). Stator current induced harmonics were investigated for fault conditions and advanced signal analysis involved continuous and discrete wavelet transforms. Simulation and experimental results are presented to substantiate that the proposed method worked over a wide speed range for motor operation and that it provided an effective tool for diagnosing PMSM operating condition.

Keywords: permanent magnet synchronous motor (PMSM), condition monitoring, fault diagnosis, eccentricity, demagnetisation, wavelet analysis, finite elements analysis (FEA).

Received: April 11th 2011
Accepted: March 2nd 2012

Introduction

Permanent magnet synchronous motors (PMSM) are becoming popular in high-performance applications compared to other types of AC motors. High-speed operation and precise torque control are some advantageous features including high torque to current ratio and high power to weight ratio, high efficiency, low noise and robustness.

Drive failure in many applications has a serious impact on system operation; such failure sometimes results in lost production or may jeopardise human safety. For instance, flight control actuation systems are a critical subsystem in aerospace vehicles. Actuation system faults can endanger operational safety and prevent an intended operation being accomplished. Detecting faults in an actuation system is essential for initiating maintenance action to prevent total system failure (Cao *et al*., 2011; Ertugrul *et al*., 2001). PMSM condition monitoring and fault detection and diagnosis have thus received growing attention amongst scientists and engineers during the last years.

The range of faults in PMSM machines includes electromechanical faults, such as short circuits and demagnetisation, and mechanical faults such as rotor eccentricity and bearing damage. Machine eccentricity appears when there is an unequal air gap between rotor and stator. Two kinds of eccentricity can be considered; static and dynamic. The minimum air gap location appears at a specific position fixed in space in static eccentricity whilst dynamic

[1] Electrical Engineer, Universidad del Valle, Colombia. PhD in Electronic Engineering, Universidad Politécnica de Cataluña, Spain. Electrical Machines & Drives Group (EM&D), Departamento de Ingeniería Eléctrica y Electrónica, Universidad Nacional de Colombia. E-mail: jaroserog@unal.edu.co
[2] Electrical Engineer, Universidad Politécnica de Cataluña, Spain. PhD in Electronic Engineering, Universidad Politécnica de Cataluña, Spain. E-mail: romeral@el.upc.du
[3] Mechanical Engineering, Universidad del Valle, Colombia. MSc in Automatization, Universidad del Valle, Colombia. E-mail: emilros@univalle.edu.co

eccentricity exists when the minimum air gap location changes with the rotor's angular position and revolves with it. By considering a low level of static eccentricity which is usual in precise machine manufacturing, (dynamic) eccentricity appears during machine operation due to bearing misalignment, mechanical resonance at critical speeds, a bent rotor shaft, bearing wear and other causes (Sundaram & Toliyat, 2011; Rosero *et al*., 2006). Mechanical rotor imbalance and rotor eccentricity are reflected in electromagnetic quantities, especially in flux, and hence in electrical and mechanical quantities (Kral *et al*., 2004).

Motor current signature analysis (MCSA) of eccentricity fault detection in an induction motor (IM) is one of the more useful methods for detecting this kind of fault in an IM running in dynamic condition (Nandi *et al*., 2012). The MCSA concept can be extended to PMSM where mean rotor harmonics and multiples show eccentricity, especially for 1st, 3rd, 5th and 7th rotor frequency (Ferrah *et al*., 1997; Le Roux *et al*., 2003; Hajiaghajani *et al*., 2003); eccentricity and varying load torque at rotor speed frequency influence stator current in much the same way. However, electromagnetic torque can also be used to distinguish between rotor fault and varying load torque by increasing on-line speed-controller bandwidth (Le Roux *et al*., 2007). However, a motor usually operates in a non-stationary environment and a motor's state variables (i.e. current, torque and speed) change as time elapses. Fault harmonics' position changes in such variable conditions as time elapses and classical FFT cannot be applied, because time information is lost in transforming to the frequency domain and the event becomes masked by the transformation.

J. S. Hsu and J. Stein analysed dynamic eccentricity detection in brushless DC motors operating in variable conditions (Hsu & Stein, 1994). However, none of the previous methods can be used when a motor is operating continuously in non-stationary state.

Wavelet analysis attempts to solve these problems by simultaneously decomposing a time series into time/frequency space. Wavelet analysis breaks a signal up into shifted and scaled versions of the original (or mother) wavelet, this being wavelet analysis' real advantage over a moving Fourier spectrum. It should be pointed out that wavelet analysis always uses a wavelet of exactly the same shape, only the size scales up or down with the size of the window. Analytic wavelet transform of the stator-current signal has been proposed for detecting dynamic eccentricity in brushless direct current (BLDC) motors operating in rapidly varying speed and load conditions (Rajagopalan *et al*., 2007).

This paper has investigated the effects of dynamic eccentricity on PMSM machines through both simulations and experiments. A PMSM stator current running with speed variations is analysed by continuous (CWT) and discrete wavelet transform (DWT).

Analysing faulty electrical machines by finite elements analysis

Analysing and developing fault detection methods requires a good knowledge of motor behaviour in fault conditions. Electrical variables, such as current and flux, or mechanical ones, such as torque or speed, are the usual signals considered in fault analysis. Models of faulty electric motors are the usual tools for acquiring electromechanical fault signals which are usually represented as time evolution signals or specific harmonics due to faults if stationary conditions can be assumed. Compact parametric models of the motor are used if a motor is considered to be in a healthy state, i.e. to calculate efficiency, obtain torque-speed relationship, analyse and develop control algorithms, etc. However, it is difficult to model faults in specific parts of a motor by means of parameters; simulations using finite element analysis (FEA) can be used to overcome this drawback. FEA is the best choice for solving partial differential equations in complex domains when the domain changes (as during a fault), or when the main objective concerns final results, and there is no interest in the procedure or the tool (Faiz *et al*., 2010a). FEA is an accurate and easy method for determining non-linear magnetic effects' interaction with non-linear electric circuits in fault conditions (Bouji et al., 2001).

PMSM in eccentricity

Assuming the infinitely permeable characteristic of ferromagnetic materials, a rotating sinusoidal magnetomotive force (MMF) is only accountable for air gaps. Excitation MMFs for individual poles are the same because the stator winding is connected in series (Hsu & Stein, 1994). Air gap MMF amplitude remains uniform regardless of air gap variation.

$$F_{mm} = A\sin\left(p_n\theta \pm 2\pi\, f_s\, t\right) = A\sin\left(p_n\theta \pm w_s\, t\right) \qquad (1)$$

where A is MMF amplitude, t is time, θ is the angular position of rotor, $P_n = up$, and u is the number of harmonics (6k ± 1) induced in the rotor flux by stator MMF space harmonics (slot) and p is a pair of poles.

Air gap flux density is proportional to the ratio of MMF air gap to air gap length. Even with an MMF air gap of uniform amplitude, air gap length variations caused by eccentricity, slot openings, salient pole faces, etc., produce a non-sinusoidal air gap flux. Its frequency is basically fundamental but with harmonics. More harmonic fluxes would be produced when stator windings are fed unbalanced phase currents producing negative-sequence rotating fields, or when magnetic saturation occurs.

The flux linkages become displaced because eccentricity modifies the air gap; the higher the eccentricity, the less the flux penetration in the rotor. On the contrary, the less the eccentricity, the higher the flux linkage and the flux penetrates deeply into a rotor's core. Flux displacement provokes a higher armature reaction in half of the magnetic pole and the flux concentrates in the minimum air gap having maximum density in the slot's head. The specific permeance function (Faiz *et al*., 2010a; Faiz *et al*., 2010b) with static and dynamic eccentricity can be expressed as:

$$P \approx P_O + P_1\cos\left(\theta\right) + P_2\cos\left(\theta - \omega_r\, t\right) \qquad (2)$$

where PO is the average part of the said function, P1 and P2 are the peaks of static and dynamic eccentricity, respectively.

Rotor MMF generated by the interaction of (1) with a type of eccentricity must interact with the other type of eccentricity to produce all low-frequency components. Consider the components of air-gap flux density produced by the interaction of (1) only with the static eccentricity component of (2). Regarding the stator, then:

$$B_{se} = \frac{AP_1}{2}\sin\left[\left(p_n \mp 1\right)\theta \pm \omega_s\, t\right] \qquad (3)$$

The flux density components of (3) induce voltages in the rotor. These induced voltages cause rotor currents to generate corresponding rotor MMFs. The interaction of these rotor MMFs with the dynamic eccentricity component of (2) produce air-gap flux density components such as.

$$B_{se} = \frac{AP_1P_2}{4}\sin\left[\left(p_n \mp 2\right)\theta \pm \left(\omega_s \pm \omega_r\right)t\right] \qquad (4)$$

Expression (4) clearly shows that extra stator current components are introduced at $w_s \pm w_r$. Some components of air-gap flux density produced by the interaction of (3) first with only the dynamic eccentricity component of (2) and later with the static eccentricity component of (3) also induce stator currents at $w_s \pm w_r$. These components produce additional ($R \pm P_n$) pole pair rotor MMF harmonics at frequency $[R(\theta \pm \omega_r t)]$, which combine with static and dynamic eccentricity components (4), giving:

$$B_{ser} = A_R \sin\left[\left[p_n \pm R \pm 2\right]\theta \pm \left(\frac{(1-s)}{p}(R \pm 1) \pm 1\right)w_s t\right] \qquad (5)$$

Interaction between flux and permeability with an eccentricity fault can be seen in Figure 1 and Figure 2. The flux density components so defined will induce voltage in the stator and this will produce high-frequency stator current components. The more representative flux density harmonics for eccentricity are expressed by (5) and usually correspond to a stator's main harmonics at (6k ± 1) for electrical machines. These harmonics are added or subtracted from to rotor speed according to the harmonics' rotational direction (positive or negative rotation).

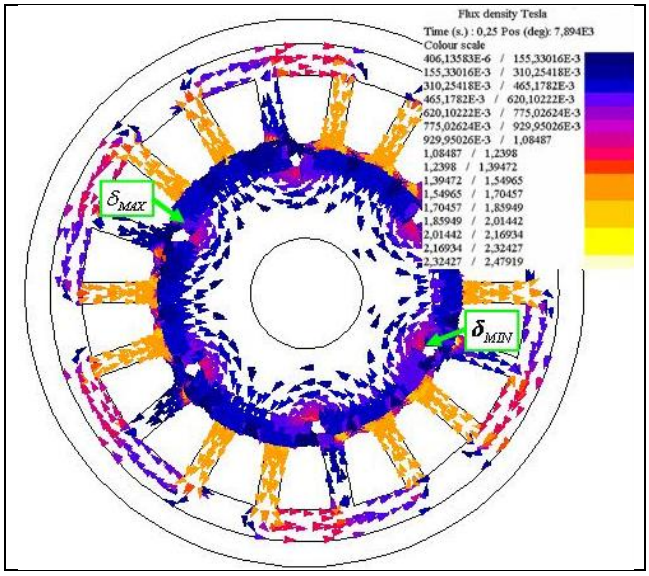

Figure 1. PMSM flux linkages at 50% dynamic eccentricity

Equation (5) can be adapted for diagnosing PMSM by $s=0$. The flux density spectrum for a PMSM with eccentricity is shown in Figure 3. Flux density 2nd, 6th, 10th and 18th harmonics are the largest and they will affect stator current harmonics.

Figure 4 shows stator current harmonics for a PMSM with eccentricity. It is shown that 1st, 5th, 7th, 11th and 13th harmonics' amplitudes are higher than in a healthy PMSM. High values for stator currents' 5th and 7th main harmonics (rotor frequency 15th and 21st harmonics) were obtained in simulations.

This was because relative inclination between stator slots and permanent magnets were not considered in simulations and the winding was concentrated. Nor was winding isolation included in the model because it would have increased the number of nodes and simulation time. It should be kept in mind that the previous considerations did not significantly affect FEA transitory analysis. Failure can be observed in experimental test 1st, 5th and 11th harmonics carried out at 50% eccentricity.

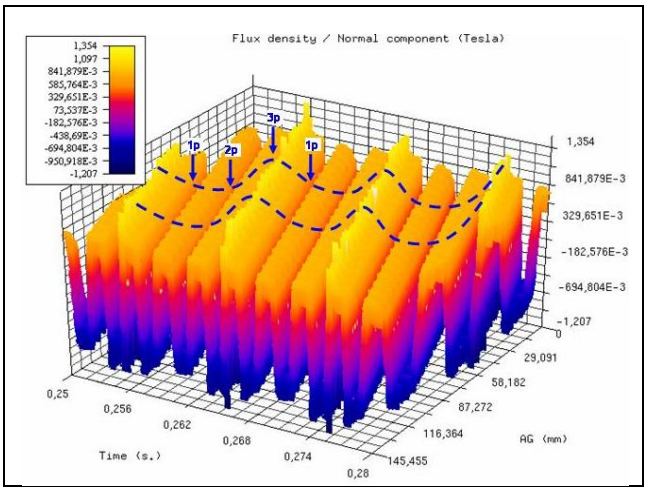

Figure 2. PMSM flux density in air gap at 50% dynamic eccentricity

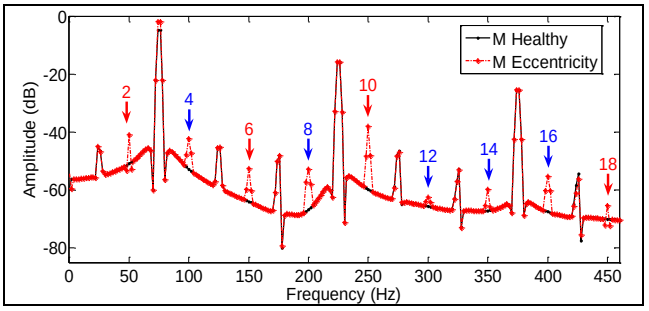

Figure 3. Flux density spectrum for PMSM with eccentricity

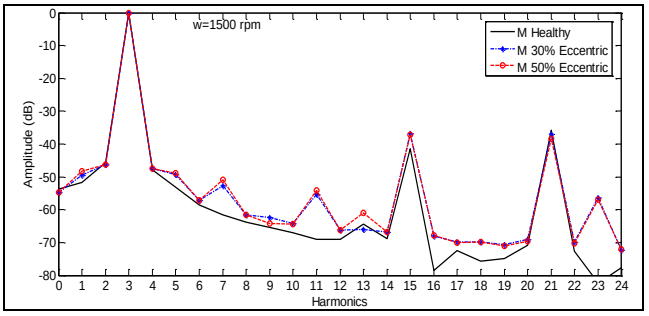

Figure 4. Stator current harmonics for a PMSM with eccentricity. Simulations made at 1,500 rpm.

Wavelet transform

The main advantage of wavelet over short-time Fourier transform (STFT) is that it uses a variable-sized-regions windowing technique (Mohammed *et al.*, 2006). Wavelet analysis can reveal aspects of data that other signal analysis techniques miss, like trends, breakdown points and discontinuity in higher derivatives. It also allows denoising signals and chooses bands to focus analysis by using mother wavelet function and scaling function wavelet (Mallat, 1998; Aller *et al.*, 2002). The wavelet approach is essentially an adjustable window Fourier spectral analysis.

Wavelet transform decomposes signals over dilated and translated wavelets. It is normalised so that $||\psi|| = 1$, and centred close to t

= 0. A family of time-frequency atoms is dilated with scale parameter s, and translated by u:

$$\psi_{u,s}(t) = \frac{1}{\sqrt{s}}\psi\left(\frac{t-u}{s}\right) \quad (6)$$

The following definition (Mallat, 1998) is the continuous wavelet transform (CWT) of signal f(t) at time u and scale s:

$$Wf(u,s) = \int_{-\infty}^{+\infty} X(t)\frac{1}{\sqrt{s}}\psi^*\left(\frac{t-u}{s}\right)\partial t \quad (7)$$

where, ψ(t) is mother wavelet function.

Although time and frequency do not explicitly appear in the transformed result, variable *1/s* gives the frequency scale and u an event's temporal location. An intuitive physical explanation of (7) is very simple: Wf(u,s) is the ´energy´ of X for scale s at t = u.

Dilation and translation parameters in discrete wavelet transform (DWT) are only restricted to discrete values. Digital signal processing leads to obtaining wavelet transform coefficients W(s,u), on a discrete grid of discrete time wavelet coefficients. This is achieved when s and u are assigned regularly spaced values (Cade *et al*., 2005): $s=ms_o$ and $u=nu_o$, where *m* and *n* are integer values. The scale is sampled along a dyadic sequence (2^n) to simplify numerical calculations.

DWT is computed by successive low-pass and high-pass filtering of discrete time-domain signal together with changes in sampling rates. A signal can be successively approximated by details having different scales.

The information obtained from CWT is redundant. Algorithms must be defined to extract the main features to reduce the amount of data and obtain quality parameters (i.e. the ridges algorithm is a good choice). This algorithm can be applied to any time-frequency transform and it obtains local maxima medium value in spectrum decomposition for every Δt considered. The calculated parameter's time evolution is a good tool for diagnostic purposes (Aller *et al*., 2002; Buckheit *et al*., 2005).

Simulation and experimental results

A 3-pair pole PMSM (2.3 Nm, 230 VAC, 6,000 rpm) was used in simulations and experiments. The faulty motor was simulated at different speeds using 2-D FEA. Numerical simulations combined FEA software Flux2D for the motor model and electric circuit and Matlab-Simulink for simulating power electronics and control. The PMSM had i_d=0 current loop and a PID speed control loop. Electromagnetic and electric circuits were automatically coupled by linking local variations in flux with circuit voltage. Eccentricity was measured as the relationship between rotor or stator displacement from centre and air gap normal longitude. Experiments were carried out for motors having different levels of eccentricity; the motors were driven at nominal, medium and low speed and 30% and 50% dynamic eccentricity were considered for the simulations, whereas 50% eccentricity was checked in the experiments; ±500 rpm speed variations, 7.5 rpm/milisec slope, were introduced during the experiments. A 2.3 N.m constant load was considered for the simulations and imposed during experiments. As typical eccentricity tolerance during motor manufacture is about 10%, such eccentricity could be considered normal and represented realistic motor damage during normal operation. All the information shown on the spectrum was normalised to rotor frequency for every simulation and experiment.

Matlab was used for wavelet transform and AWT ridges algorithm using the Wavelab850 toolbox from Stanford University which has been also used by other authors (Buckheit *et al*., 2005).

Continuous wavelet transforms (CWT).

Figure 5 illustrates CWT results for PMSM with eccentricity. Clearer lines in indexes 118-131 and 157-170 represented high amplitude harmonics. These lines did not appear in a healthy machine. The CWT was more visible and easier to understand and was used to evaluate PMSM eccentricity. The results depicted in the figure were obtained from PMSM simulation having 50% eccentricity with the motor running at high speed. Local maximums using the ridges method were calculated from the previous CWT. This algorithm looked for the most important values in time

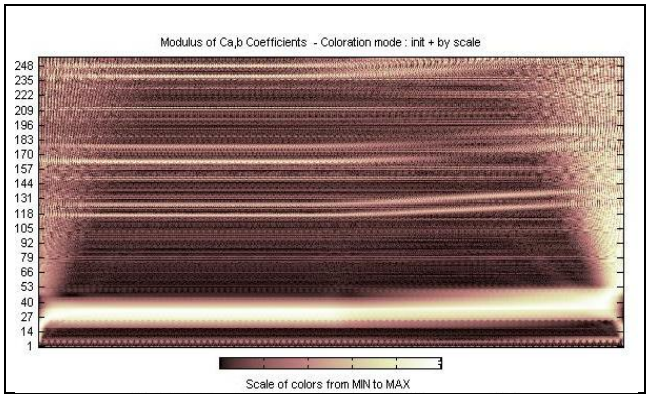

Figure 5. CWT for PMSM with eccentricity, speed changes from 6,000 to 5,500 rpm, simulation results of PMSM with eccentricity

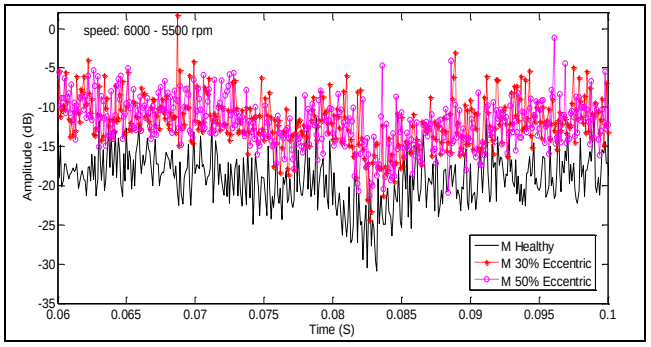

Figure 6. Average ridges CWT, speed changes from 6,000 to 5,500 rpm, simulation results for PMSM with eccentricity

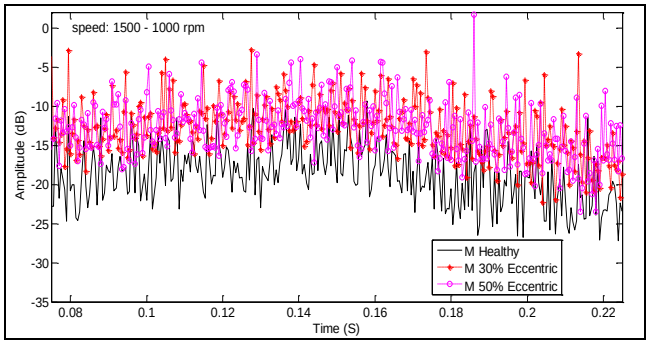

Fig. 7. Average eidges CWT, speed changes from 1,500 to 1,000 rpm, simulation results of PMSM with eccentricity

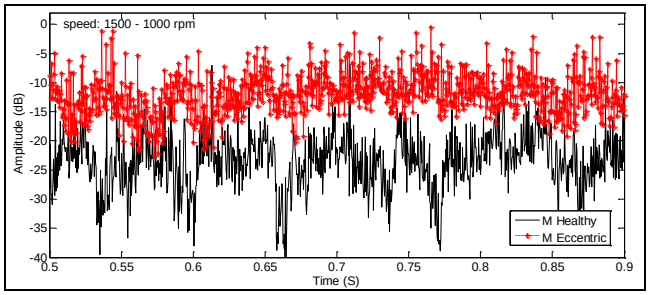

Figure 8. Average ridges CWT, speed change from 1,500 rpm to 1,000 rpm, experimental results of PMSM uwith eccentricity

and frequency ranges. Local maximums were averaged and compared to those obtained for a healthy machine to obtain a representative fault parameter. Figure 6 and Fig. 7 illustrate these CWT averaged ridge values. They were obtained from high and low speed simulations. A difference of ±7 dB was obtained in the values obtained for an eccentric motor and a healthy one, at both-low and high speeds. Experimental results confirmed simulations (Figure 8.) CWT thus distinguished eccentricity faults, even regarding speed variation, while preserving nice resolution for low speeds. A 20% to 100% torque variation was also considered.

The 6 dB difference found between healthy and faulty machines demonstrated that CWT also identified eccentricity in torque variations. There were no appreciable differences in torque and speed variation results (i.e. CWT led to evaluating eccentricity level and thus diagnosed the state of the machine in all conditions).

DWT

A DWT stator current motor analysis was carried out for speed changes at nominal torque. The 7-level DWT Meyer was used. The energy for every detail was obtained to evaluate a faulty machine. Tables 1 and 2 show the energy for every detail and approximation coefficients for a DWT applied to stator currents obtained from simulations and experiment tests (Rosero *et al*., 2007). Table 1 shows details 2, 3, 5 and 6 as being the most promising for identifying failure for a PMSM running at 6,000 rpm. DWT detail 2 had the 7th and 11th harmonics, detail 5 included the 1st harmonic

Table 1. Energy of detail and approximation coefficients for DWT. PMSM stator current DWT Meyer (7). Simulated results

6,000 rpm. 300 Hz.					
Type	**A7**	**D2**	**D3**	**D5**	**D6**
Healthy motor	0.34	0.22	0.42	0.89	0.67
M30% eccentricity	1.15	0.91	0.39	1.28	1.36
M50% eccentricity	1,12	0.85	0.41	1.27	1.39
3,000 rpm. 150 Hz.					
Type	**A7**	**D3**	**D4**	**D6**	
Healthy motor	0.29	0.51	0.79	0.48	
M30% eccentricity	1.05	1.09	0.81	1.29	
M50% eccentricity	1.12	1.10	0.83	1.35	
1,500 rpm. 75 Hz.					
Type	**A7**	**D4**	**D7**	**--**	
Healthy motor	0.35	0.69	0.22	--	
M30% eccentricity	1.06	1.22	0.52	--	
M50% eccentricity	1.10	1.19	0.53	--	

Table 2. Energy of detail and approximation coefficients for DWT. PMSM stator current DWT Meyer (7). Simulated results

6,000 rpm. 300 Hz.					
Type	**A7**	**D2**	**D3**	**D5**	**D6**
Healthy motor	0.23	0.36	0.71	0.39	0.55
M40% eccentricity	1.25	1.16	0.69	0.77	1.08
3,000 rpm. 150 Hz.					
Type	A7	D3	D4	D6	
Healthy motor	0.32	0.29	0.62	0.43	
M40% eccentricity	1.10	0.85	0.65	0.85	
1,500 rpm. 75 Hz.					
Type	A7	D4	D7	--	
Healthy motor	0.28	0.20	0.21	--	
M40% eccentricity	0.21	0.65	0.51	--	

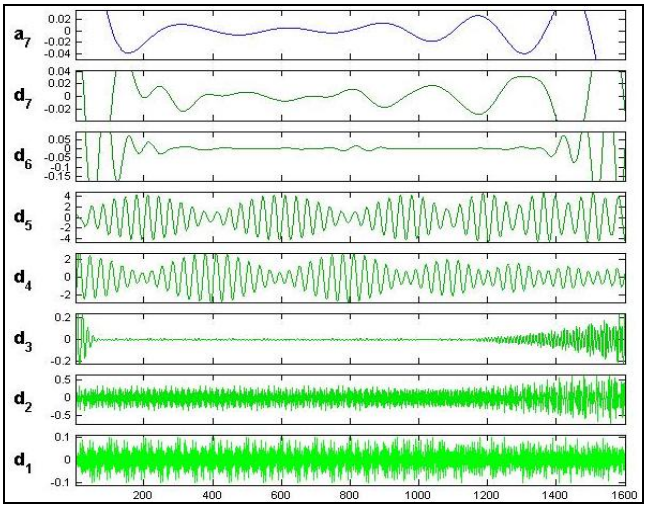

Fig. 9. DWT for healthy PMSM, speed changes from 6,000 rpm to 5,500 rpm, simulation results

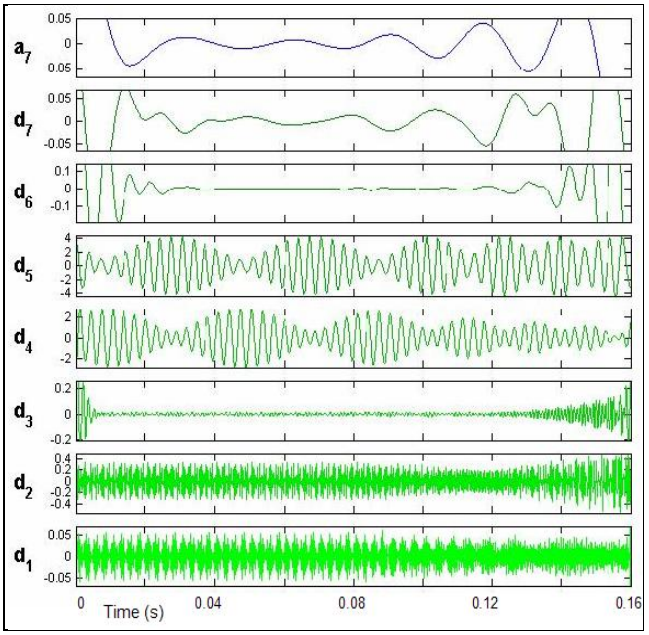

Fig. 10. DWT for PMSM with 50% eccentricity, speed changes from 6,000 to 5,500 rpm, simulation

and detail 3 the 5th harmonic. Simulations and experimental results were obtained for 1,500 rpm and 3,000 rpm. It was observed that the most interesting details were the same as or close to those found at 6,000 rpm. In any case, there was always at least one detail containing information about the failure for every speed. DWT thus detected faults at high, medium and low speeds. Details agreed with sample frequency and rotation speed. Detail wave forms are shown in Fig. 9 and 10; they were obtained from simulation results having the same form in experimental results.

Conclusions

The finite elements analysis method (FEA) was used to analyse eccentricity in this paper.

Continuous wavelet transform led to detecting eccentricity visually and a numerical indication of failure was obtained by using the ridge algorithm and averaging the results, even for a speed as low as ± 600 rpm.

The discrete wavelet transform evaluated failure by calculating details' energy. The appropriate choice of interest detail depended on PMSM sample frequency and rotation speed. DWT analysed and identified faults by means of stator current, even at high, medium and low speed.

This algorithm was shown to be an excellent tool for eccentricity and demagnetisation fault detection in PMSM motors, regardless of speed and torque variations.

The proposed method's validity was confirmed by the experimental result.

References

Aller J. M., Habetler T. G., Harley R. G., Tallam R. M., Sang Bin L., Sensorless speed measurement of AC machines using analytic wavelet transform, IEEE Transactions on Industry Applications, vol. 38, 2002, pp. 1344-1350.

Bouji M., Arkadan A. A., Ericsen B. T., Fuzzy inference system for the characterization of SRM drives under normal and fault conditions, IEEE Transactions on Magnetics, vol. 37, issue: V, 2001pp. 3745-3748.

Buckheit J., Chen S., Donoho D., Johnstone I., Scargle J., WaveLab850 http://www-stat.stanford.edu/~wavelab vol. Version .850: Stanford University & NASA-Ames Research Center,

Cade I. S., Keogh P. S., Sahinkaya M. N., Fault identification in rotor/magnetic bearing systems using discrete time wavelet coefficients, IEEE/ASME Transactions on Mechatronics, vol. 10, 2005, pp. 648-657.

Cao W., Mecrow B., Bennett B. J., Atkinson D. J., Overview of electric motor technologies used for more electric aircraft (MEA)., Transactions on Industrial Electronics, IEEE, Issue 99, 2011, pp. 1-9.

Ertugrul N., Soong W. L., Valtenbergs S., Chye H., Investigation of a fault tolerant and high performance motor drive for critical applications, in TENCON. Proceedings of IEEE Region 10 International Conference on Electrical and Electronic Technology, Vol.2, 2001, pp. 542-548.

Faiz J., Ebrahimi B. M., Akin B., Toliyat H. A., Dynamic analysis of mixed eccentricity signatures at various operating points and scrutiny of related indices for induction motors, IET Electric Power Applications, vol. 4, issue I, 2010, pp. 1-16.

Faiz J., Ebrahimi D. M., Akin B., Toliyat H. A., Dynamic analysis of mixed eccentricity signatures at various operating points and scrutiny of related indices for induction motors, IET Electric Power Applications, vol. 4, issue: 1, 2010, pp. 253-260.

Ferrah A., Hogben-Laing P. J., Bradley K. J., Asher G. M., Woolfson M. S., The effect of rotor design on sensorless speed estimation using rotor slot harmonics identified by adaptive digital filtering using the maximum likelihood approach, in 32nd IAS Annual Meeting, IAS '97., Conference Record of the Industry Applications Conference, 1997. IEEE, vol.1, 1997, pp. 128-135.

Hajiaghajani M., Lei H., Madani S. M., Toliyat H. A., A method for detection of eccentricity in permanent magnet machines, in 38th IAS Annual Meeting. Conference Record of the Industry Applications Conference, Vol.3, 2003, pp. 1833-1838.

Hsu J. S. Stein J., Effects of eccentricities on shaft signals studied through windingless rotors, IEEE Transactions on Energy Conversion, Vol. 9, 1994, pp. 564-571,.

Kral C., Habetler T. G., Harley R. G., Detection of mechanical imbalances of induction machines without spectral analysis of time-domain signals, IEEE Transactions on Industry Applications, vol. 40, 2004, pp. 1101-1106.

Le Roux W., Harley R. G., Habetler T. G., Detecting rotor faults in permanent magnet synchronous machines," in SDEMPED 2003. 4th IEEE International Symposium on Diagnostics for Electric Machines, Power Electronics and Drives, 2003, pp. 198-203.

Le Roux W., Harley R. G., Habetler T. G., Detecting rotor faults in low power permanent magnet synchronous machines, Transactions on Power Electronics, Vol. 22, Issue: I, 2007, pp. 322-328.

Mallat S. G., A wavelet tour of signal processing. San Diego: Academic Press, 1998.

Mohammed O. A., Abed N. Y., Ganu S., Modeling and characterization of induction motor internal faults using finite-element and discrete wavelet transforms, IEEE Transactions on Magnetics, vol. 42, 2006, pp. 3434-3436.

Nandi S., Toliyat H. A., Li X., Performance-oriented electric motors diagnostics in modern energy conversion systems, IEEE Transactions on Industrial Electronics, vol. 59, Issue: II, 2012, p. 1266-1277.

Rajagopalan S., Aller J. M., Restrepo J. A., Habetler T. G., Harley R. G., Analytic-wavelet-ridge-based detection of dynamic eccentricity in brushless direct current (BLDC) motors functioning under dynamic operating conditions, IEEE Transactions on Industrial Electronics, vol. 54, 2007, pp. 1410-1419.

Rosero J., Cusido J., Garcia A., Ortega J. A., Romeral L., Broken bearings and eccentricity fault detection for a permanent magnet synchronous motor, in The 32nd Annual Conference of the IEEE Industrial Electronics Society, IECON06, Paris - FRANCE, 2006, pp. 964-969.

Rosero J., Romeral L., Cusido J., Ortega J. A., Fault detection by means of wavelet transform in a PMSM under demagnetization, in The 33rd Annual Conference of the IEEE Industrial Electronics Society, IECON07, Taipei, Taiwan, 2007.

Sundaram V. M., Toliyat H. A., Diagnosis and isolation of air-gap eccentricities in closed-loop controlled doubly-fed induction generators, IEEE Conference International of Electric Machines & Drives Conference (IEMDC), 15-18 May, 2011, 2011, pp. 1064-1069.